

# A Site-Isolated Rhodium–Diethylene Complex Supported on Highly Dealuminated Y Zeolite: Synthesis and Characterization

Ann J. Liang, Vinesh A. Bhirud, Justin O. Ehresmann, Philip W. Kletnieks, James F. Haw, and Bruce C. Gates\*

Department of Chemical Engineering and Materials Science, University of California, Davis, California 95616, and Department of Chemistry, University of Southern California, Los Angeles, California 90086

Received: August 16, 2005; In Final Form: October 29, 2005

The reaction of  $\text{Rh}(\text{C}_2\text{H}_4)_2(\text{acac})$  with the partially dehydroxylated surface of dealuminated zeolite Y (calcined at 773 K) and treatments of the resultant surface species in various atmospheres ( $\text{He}$ ,  $\text{CO}$ ,  $\text{H}_2$ , and  $\text{D}_2$ ) were investigated with infrared (IR), extended X-ray absorption fine structure (EXAFS), and  $^{13}\text{C}$  NMR spectroscopies. The IR spectra show that  $\text{Rh}(\text{C}_2\text{H}_4)_2(\text{acac})$  reacted readily with surface OH groups of the zeolite, leading to loss of acac ligands from the  $\text{Rh}(\text{C}_2\text{H}_4)_2(\text{acac})$  and formation of supported mononuclear rhodium complexes, confirmed by the lack of Rh–Rh contributions in the EXAFS spectra; each Rh atom was bonded on average to two oxygen atoms of the zeolite surface with a Rh–O distance of 2.19 Å. IR, EXAFS, and  $^{13}\text{C}$  NMR spectra show that the ethylene ligands remained bonded to the Rh center in the supported complex. Treatment of the sample in CO led to the formation of site-isolated  $\text{Rh}(\text{CO})_2$  complexes bonded to the zeolite. The sharpness of the  $\nu_{\text{CO}}$  bands in the IR spectrum gives evidence of a nearly uniform supported  $\text{Rh}(\text{CO})_2$  complex and, by inference, the near uniformity of the mononuclear rhodium complex with ethylene ligands from which it was formed. The supported complex with ethylene ligands reacted with  $\text{H}_2$  to give ethane, and it also catalyzed ethylene hydrogenation at 294 K.

## Introduction

Many industrial catalysts are solids that offer the advantages of ease of separation from products, lack of corrosiveness, and robustness allowing operation at high temperatures with gas-phase reactants and low pressures. Solid catalysts typically offer sites for reaction only at intrinsically nonuniform surfaces, and the corresponding spectrum of reactivities typically imposes a low selectivity in catalysis.<sup>1,2</sup> In contrast, the most successful soluble catalysts used in industry are characterized by high selectivities, associated with the unique, molecular species. In prospect, structurally simple and uniform catalysts anchored to supports offer the same selectivity advantages as molecular catalysts in solution, combined with the advantages of solids generally. Efforts to design robust, well-defined supported catalysts have led to industrial applications, exemplified by the processes for olefin polymerization catalyzed by supported metallocenes<sup>3</sup> and the Chiyoda process for methanol carbonylation to give acetic acid catalyzed by a polymer-supported rhodium carbonyl.<sup>4,5</sup>

Structural characterization of such supported molecular catalysts typically requires a combination of spectroscopic techniques, such as X-ray absorption spectroscopy and IR spectroscopy, to determine the structure of the catalytic species and account for the ligands, including the support, and the oxidation state(s) of the metal.<sup>1,2</sup> To prepare supported catalysts that are molecular analogues, one may begin with organometallic complexes and graft them to supports. For example, Copéret et al.<sup>6</sup> used  $\text{Ta}(\text{=CHtBu})(\text{CH}_2\text{tBu})_3$  to synthesize  $\text{SiO}_2$ -supported catalysts represented as  $\{\text{SiO}_2\}\text{Ta}(\text{=CHtBu})(\text{CH}_2\text{tBu})_2$  (the braces denote groups that are part of the  $\text{SiO}_2$  support), which incorporate reactive ligands and appear to be species that participate in a catalytic cycle for alkane metathesis.

Among the organometallic precursors that offer good opportunities for preparing supported catalysts are metal acetylacetonate (acac) complexes. These have been demonstrated to afford clean and relatively well understood metal complexes bonded to zeolites and metal oxides.<sup>7–9</sup> Catalysts prepared from these precursors have for the most part suffered from lack of activity associated with the relatively unreactive nature of the ligands (such as carbonyls) remaining bonded to the metal center after removal of the acac ligands and bonding of the metal to the support.

The goals of the research reported here were to prepare and characterize nearly uniform supported metal catalysts with reactive ethylene ligands. We used  $\text{Rh}(\text{C}_2\text{H}_4)_2(\text{acac})$  as the precursor to take advantage of the reactivity of the acac ligands, with the goal of retaining the ethylene ligands on the supported complex. We chose a zeolite as the support in an attempt to take advantage of its regular (crystalline) structure to prepare supported complexes in uniform sites. We report synthesis of the surface species and their characterization by extended X-ray absorption fine structure (EXAFS) spectroscopy and infrared (IR) and  $^{13}\text{C}$  NMR spectroscopies and the testing of the sample as a catalyst for a simple reaction involving ethylene ligands as potential reaction intermediates, ethylene hydrogenation. In related work,<sup>10</sup> we have prepared rhodium complexes from the same precursor on another support, dehydroxylated  $\text{MgO}$ .

## Experimental Section

**Materials and Sample Preparation.** Sample syntheses and handling were performed with the exclusion of moisture and air.  $\text{H}_2$  was supplied by Airgas (99.999%) or generated by electrolysis of water in a Balston generator (99.99%) and purified by passage through traps containing reduced  $\text{Cu}/\text{Al}_2\text{O}_3$ .

and activated zeolite 4A to remove traces of O<sub>2</sub> and moisture, respectively. He (Airgas, 99.999%) and C<sub>2</sub>H<sub>4</sub> (Airgas, 99.99%) were purified by passage through similar traps. CO (Matheson, 99.999%), in a 10% mixture in He, was purified by passage through a trap containing activated  $\gamma$ -Al<sub>2</sub>O<sub>3</sub> particles and zeolite 4A to remove any traces of metal carbonyls from high-pressure gas cylinders and moisture, respectively. Ethylene-2-<sup>13</sup>C (99% <sup>13</sup>C) was purchased from Cambridge Isotopes. The highly dealuminated HY zeolite (DAY zeolite) (Zeolyst International), with a Si/Al atomic ratio of  $\sim$ 30, was calcined in O<sub>2</sub> at 773 K for 4 h and evacuated for 16 h at 773 K, isolated, and stored in a Vacuum Atmospheres HE-63-P N<sub>2</sub>-filled glovebox until it was used. *n*-Pentane solvent (Fisher, 99%) was dried and purified by refluxing over sodium benzophenone ketyl and deoxygenated by sparging with nitrogen. The precursor Rh(C<sub>2</sub>H<sub>4</sub>)<sub>2</sub>(C<sub>5</sub>H<sub>7</sub>O<sub>2</sub>) [acetylacetonatobis(ethylene)rhodium(I)] (Strem, 99%) and the reference compound acetylacetone (Hacac) (Sigma-Aldrich, 99%) were used as supplied.

To prepare the supported rhodium complex, Rh(C<sub>2</sub>H<sub>4</sub>)<sub>2</sub>(acac) (acac = C<sub>5</sub>H<sub>7</sub>O<sub>2</sub>), combined with the calcined zeolite in a Schlenk flask, was slurried in dried *n*-pentane at 200 K for 1 day. The solvent was then removed by evacuation for 1 day, so that all the rhodium remained in the zeolite. The resultant powder, containing 1 wt % Rh, was pale yellow. It was stored in a glovebox.

The reaction of Hacac with DAY zeolite powder was carried out in *n*-pentane with exclusion of air and moisture; the slurry was stirred for 1 day and the solvent removed by evacuation for 1 day.

**Infrared Spectroscopy.** A Bruker IFS 66v spectrometer with a spectral resolution of 4 cm<sup>-1</sup> was used to collect transmission IR spectra of powder samples. Approximately 1 mg of powder was pressed between two KBr windows for optical optimization that allowed detection of minor peaks. All samples were handled with exclusion of moisture and air. Each spectrum represents the average of 64 scans.

In some IR experiments, the sample was present in a cell with reactive gases flowing through it. Each sample (typically, 15 mg) was pressed into a thin wafer and loaded into the cell (In-situ Research Institute, Inc., South Bend, IN) in the N<sub>2</sub>-filled glovebox. The cell was connected to a vacuum system with a base pressure of 10<sup>-4</sup> Torr, which allowed recording of spectra while the reactant gases (CO, D<sub>2</sub>, H<sub>2</sub>, and/or C<sub>2</sub>H<sub>4</sub>) flowed through the cell at the reaction temperature. Each spectrum is the average of 128 scans.

**Nuclear Magnetic Resonance Spectroscopy.** All samples were prepared with a shallow-bed CAVERN apparatus.<sup>11</sup> Typically, 0.3 g of sample in a glovebox was loaded into the CAVERN, which was removed and connected to a vacuum line. The sample was evacuated to a final pressure of less than 5  $\times$  10<sup>-5</sup> Torr. Adsorption of ethylene-2-<sup>13</sup>C and of <sup>13</sup>CO was carried out at room temperature and pressures less than 1.5 Torr to minimize any support-catalyzed side reactions. Samples were loaded into 7.5 mm zirconia rotors after adsorption of the ethylene, and the rotor was capped within the CAVERN.

Conventional <sup>13</sup>C CP/MAS and Bloch Decay MAS NMR spectra were acquired with a Chemagnetics CMX 300 (7.05 T) spectrometer equipped with a modified Chemagnetics 7.5 mm MAS probe. The sample spectrum was referenced to that of the secondary standard hexamethylbenzene (methyl signal 17.35 ppm relative to TMS); the hexamethylbenzene sample was also used to calibrate the 90° flip for both carbon and proton. Cross-polarization spectra were acquired with 2000 scans and a half-second pulse delay. Bloch decay spectra were acquired with

20 000 scans and a 10 s pulse delay. The MAS spinning speed was 5.0 kHz. The spectrum reported was recorded at 153 K rather than higher temperatures to eliminate possible consequences of ethylene rotation and to provide high sensitivity.

**X-ray Absorption Spectroscopy.** EXAFS spectra were collected at beamline X-18B at the National Synchrotron Light Source (NSLS), Brookhaven National Laboratory, Upton, NY, and at beamline 2-3 at the Stanford Synchrotron Radiation Laboratory (SSRL), Stanford Linear Accelerator Center, Stanford, CA. The storage ring electron energy was 2.8 GeV at NSLS and 3 GeV at SSRL. The ring currents were 110–250 and 50–100 mA at NSLS and SSRL, respectively.

In a glovebox at each synchrotron (filled with either argon or N<sub>2</sub>), powder samples were loaded into an EXAFS cell.<sup>12</sup> After removal from the glovebox, the cell was evacuated to a pressure less than 10<sup>-5</sup> Torr and then aligned in the X-ray beam. Spectra were collected in transmission mode at the Rh K edge (23 220 eV) with the sample at liquid-nitrogen temperature. In some experiments, spectra were collected at 298 K during treatment of the sample in flowing He, H<sub>2</sub>, and/or C<sub>2</sub>H<sub>4</sub> in the EXAFS cell described elsewhere.<sup>13</sup>

**Ethylene Hydrogenation Catalysis in a Tubular Plug-Flow Reactor.** Ethylene hydrogenation catalysis was carried out in a once-through tubular plug-flow reactor at room temperature (approximately 298 K) and atmospheric pressure. The catalyst, diluted with inert, nonporous  $\alpha$ -Al<sub>2</sub>O<sub>3</sub> in a ratio of 1:30, was loaded into the reactor in a glovebox. The catalyst was held in the middle of the reactor by glass wool plugs. The loaded reactor, after removal from the glovebox, was installed in the flow system to minimize contact of the catalyst with moisture or air. An on-line gas chromatograph (Hewlett-Packard, HP-5890 series II) equipped with a 30 m  $\times$  0.53 mm DB-624 (J & W Scientific) capillary column (with N<sub>2</sub> as the carrier gas), and a flame-ionization detector was used to analyze the reaction products. Conversions of ethylene to ethane were less than 5%, and the reactor is inferred to have operated in the differential mode, determining reaction rates directly.

The total feed flow rate (He + H<sub>2</sub> + ethylene) was typically 100 mL (NTP) min<sup>-1</sup>. Under these conditions, the reactor was well approximated as an isothermal plug-flow reactor. The reaction experiments were carried out with an ethylene partial pressure of 30 Torr and a H<sub>2</sub> partial pressure in the range of 30–300 Torr at 294  $\pm$  1 K. All catalytic results are reported for the reaction taking place at steady state, following an induction period of typically about 18 h.

**EXAFS Data Analysis.** The X-ray absorption edge energy was calibrated with the measured signal of a rhodium foil (at the Rh K edge (23 220 eV)) that was scanned simultaneously with the sample. The edge is represented as the inflection point at the first absorption peak at 23 220 eV. The data were normalized by dividing the absorption intensity by the height of the absorption edge.

Analysis of the EXAFS data was carried out with the software ATHENA from the IFEFFIT package<sup>14</sup> and the software XDAP.<sup>15</sup> Reference files, prepared either experimentally from EXAFS data representing materials of known structure or calculated by using the code FEFF7.0,<sup>16</sup> were used in the analysis. EXAFS data characterizing a rhodium foil and Rh<sub>2</sub>O<sub>3</sub> were used for the phase shifts and backscattering amplitudes of the Rh–Rh and Rh–O<sub>support</sub> interactions. Ru<sub>3</sub>(CO)<sub>12</sub>, mixed with BN, was used to obtain the phase shifts and backscattering amplitudes used in analyzing the Rh–C interaction. The transferability of the phase shifts and backscattering amplitudes for neighboring atoms in the periodic table has been justified

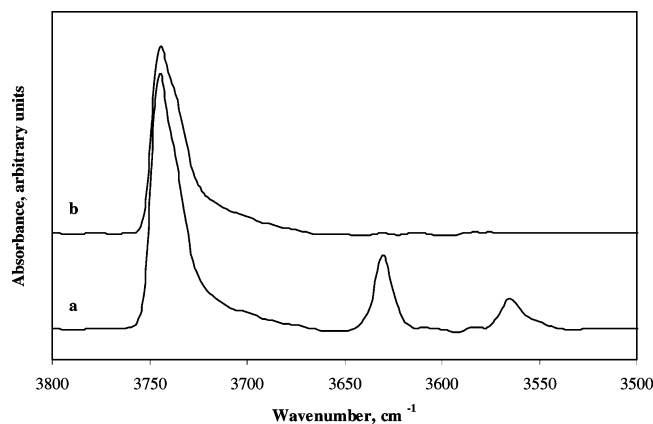


**Figure 1.** IR spectra in the  $\nu_{\text{OH}}$  region characterizing the following samples: (a) bare, partially dehydroxylated DAY zeolite; (b) sample formed by reaction of DAY zeolite with  $\text{Rh}(\text{C}_2\text{H}_4)_2(\text{acac})$  in *n*-pentane after removal of the solvent.

experimentally.<sup>17</sup> The Rh–Al reference file was calculated by using the code FEFF7.0 and structural parameters representing a Rh–Al alloy.

ATHENA was used for edge calibration, deglitching, data normalization, and conversion of the data into a chi file. XDAP allowed the efficient application of a difference-file technique<sup>18–20</sup> for the determination of optimized fit parameters. No attempt was made in the fitting to account for the small atomic X-ray absorption fine structure. Iterative fitting was carried out until good agreement was attained between the calculated  $k^0$ -,  $k^1$ -, and  $k^2$ -weighted EXAFS data and the postulated model. Plots showing the residuals remaining after the fitting are shown in the Supporting Information.

The fitting ranges in both momentum ( $k$ ) and real ( $r$ ) space ( $k$  is the wave vector and  $r$  is distance from the absorbing atom) were determined by the data quality; the range in  $k$  was 3.85–14.75  $\text{\AA}^{-1}$ , and the range in  $r$  was 1.0–4.0  $\text{\AA}$ ; these values were used with the Nyquist theorem<sup>21</sup> to compute the justified number of fitting parameters (21)). The number of parameters used in fitting the data to each model (16) was always less than this statistically justified number. The accuracies of these parameters are estimated to be as follows (with the exception of the Rh–Al contribution): coordination number  $N$ ,  $\pm 20\%$ ; distance  $R$ ,  $\pm 0.02$   $\text{\AA}$ ; Debye–Waller factor  $\Delta\sigma^2$ ,  $\pm 20\%$ ; and inner potential correction  $\Delta E_0$ ,  $\pm 20\%$ . The Rh–Al contribution is assigned only tentatively, and the errors are larger than those stated above.

We emphasize that an attempt was made to include a Rh–Rh contribution in the fit (even with a  $k^3$  weighting of the data), but none was found.

## Results

**IR Spectra Characterizing  $\nu(\text{OH})$  Region.** The IR spectra characterizing the  $\nu_{\text{OH}}$  region of DAY zeolite before and after interaction with  $\text{Rh}(\text{C}_2\text{H}_4)_2(\text{acac})$  are shown in Figure 1. The spectrum representing DAY zeolite that had been treated under vacuum at 773 K includes bands at 3745, 3629, and 3564  $\text{cm}^{-1}$ . The band at 3745  $\text{cm}^{-1}$  is assigned to terminal silanol groups, and the other two are assigned to weakly acidic hydroxyl groups.<sup>22</sup> The intensities of the bands associated with all three of these OH groups decreased after reaction of  $\text{Rh}(\text{C}_2\text{H}_4)_2(\text{acac})$  with the zeolite, indicating that OH groups were converted in the reaction with  $\text{Rh}(\text{C}_2\text{H}_4)_2(\text{acac})$ ; the peaks at 3629 and 3564  $\text{cm}^{-1}$  nearly disappeared as a result of the reaction of the support with  $\text{Rh}(\text{C}_2\text{H}_4)_2(\text{acac})$ , but the peak at 3745  $\text{cm}^{-1}$  did not.

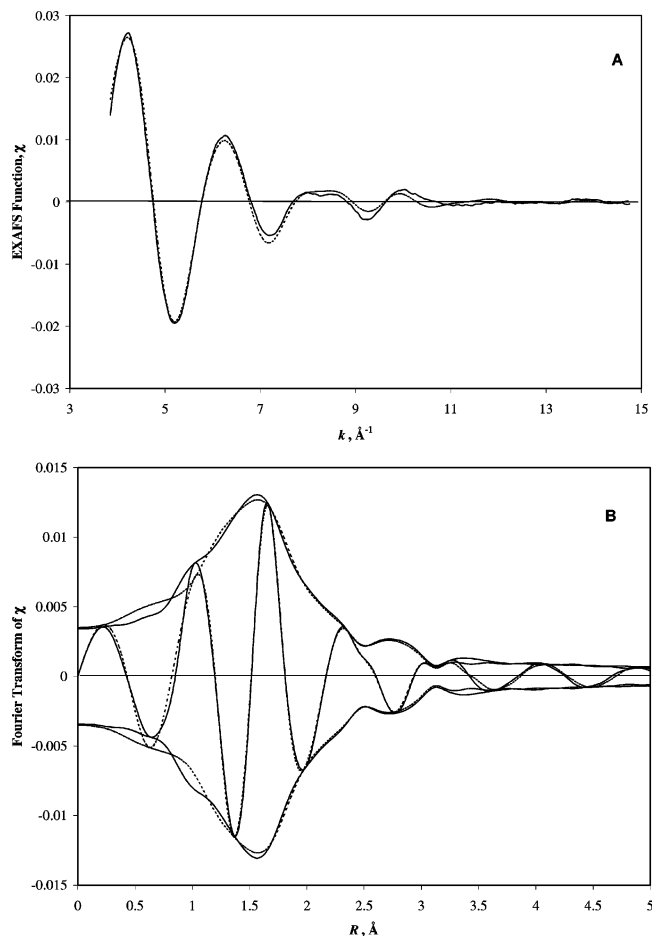


**Figure 2.** Results of EXAFS analysis characterizing the sample formed from the reaction of  $\text{Rh}(\text{C}_2\text{H}_4)_2(\text{acac})$  with DAY zeolite. (A) EXAFS function,  $\chi$  (solid line), and calculated contribution (dotted line). (B) Imaginary part and magnitude of the Fourier transform of data (solid lines), and calculated contributions (dotted lines) (unweighted,  $\Delta k = 3.85\text{--}14.75$   $\text{\AA}^{-1}$ ).

**TABLE 1: EXAFS Fit Parameters Characterizing DAY Zeolite-Supported Rhodium Complex Scanned at 77 K and  $<10^{-5}$  Torr<sup>d</sup>**

shell	$N$	$R$ , $\text{\AA}$	$\Delta\sigma^2$ , $\text{\AA}^2$	$\Delta E_0$ , eV
Rh–Rh				
Rh–O	2.2	2.19	0.0067	–3.1
Rh–C	3.9	2.09	0.0035	3.2
Rh–O <sub>i</sub>	0.7	3.41	–0.0037	6.6
Rh–Al	0.4	2.92	0.0022	0.7

<sup>a</sup> Notation:  $N$ , coordination number;  $R$ , absorber–backscatter distance;  $\Delta\sigma^2$ , Debye–Waller factor relative to that of the reference compound (see text); and  $\Delta E_0$ , inner potential correction. The approximate experimental uncertainties except for the Rh–Al contribution are as follows:  $N$ ,  $\pm 20\%$ ;  $R$ ,  $\pm 1\%$ ; the errors representative of the Rh–Al contribution are greater than these and not well characterized.

**EXAFS Evidence of Mononuclear Rhodium Bonded to Zeolite.** The EXAFS data (Figure 2 and Table 1) characterizing the sample formed by adsorption of  $\text{Rh}(\text{C}_2\text{H}_4)_2(\text{acac})$  on the calcined DAY zeolite indicate that each Rh atom in the supported sample was bonded, on average, to two oxygen atoms of the support, at a distance of 2.19  $\text{\AA}$ . This is a typical distance for bonding of group 8 metal atoms to oxygen atoms of metal oxide and zeolite supports.<sup>23</sup> Because the EXAFS data give no evidence of Rh–Rh contributions (consistent with the absence of rhodium clusters), we infer the presence of site-isolated mononuclear rhodium complexes.



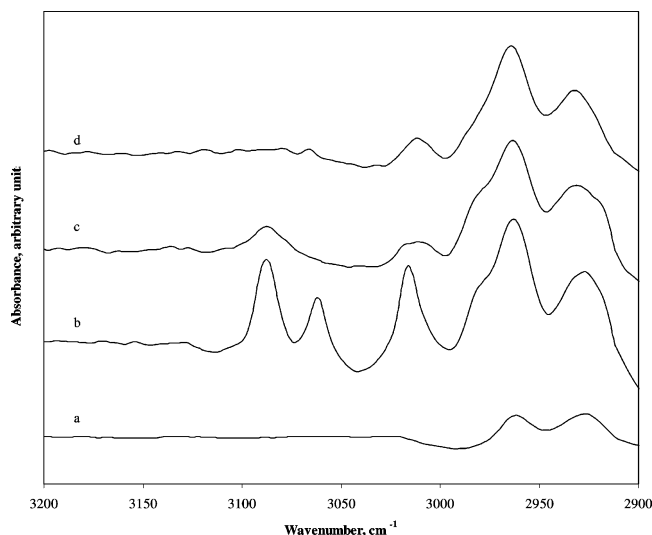


**Figure 3.** IR spectra in the  $\nu_{\text{CH}}$  region characterizing the following samples: (a) DAY zeolite calcined at 773 K, (b) sample formed by reaction of DAY zeolite with  $\text{Rh}(\text{C}_2\text{H}_4)_2(\text{acac})$ , (c) sample b treated with  $\text{H}_2$  for 30 min at 298 K, and (d) sample b after treatment with  $\text{D}_2$  at 298 K. Each spectrum was recorded with a separate wafer.

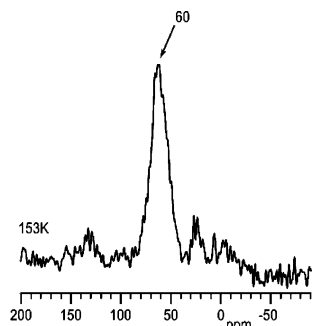


**Figure 4.** 75.4 MHz  $^{13}\text{C}$  CP/MAS NMR spectrum of the supported rhodium complex. The sample was exchanged with ethylene- $^{13}\text{C}_2$ ; hence, only one resonance, for those ligands, is observable.

The comparison of Figure 2 shows the goodness of fit of the data. Further evidence of the goodness of the fit is indicated by the residuals shown in Figure 5 in the Supporting Information.

**Evidence of Rh–C Bonds and Ethylene Ligands in Supported Complex.** The IR spectrum of the complex formed from  $\text{Rh}(\text{C}_2\text{H}_4)_2(\text{acac})$  on the zeolite that had been calcined at 773 K shows  $\nu_{\text{CH}}$  bands at 3086, 3060, 3015, and 2980  $\text{cm}^{-1}$  (Figure 3). The interpretation of this part of the spectrum is complicated because of the expected presence of  $\nu_{\text{CH}}$  contributions from the remnants of acetylacetonate ligands on the support. The peak at 3060  $\text{cm}^{-1}$  is characteristic of  $\nu_{\text{CH}}$  bands of the ethylene ligands in the supported rhodium complex as well as in the precursor  $\text{Rh}(\text{C}_2\text{H}_4)_2(\text{acac})$ .<sup>24,25</sup>

The  $^{13}\text{C}$  NMR spectrum of this sample is shown in Figure 4. The contributions from the ethylenic carbon nuclei are apparent at approximately 60 ppm, in agreement with solid-state NMR spectra of the precursor;<sup>26</sup> they provide confirming evidence of the ethylene ligands in the supported complex.<sup>27–29</sup>

The EXAFS data also support the conclusion that ethylene ligands remained bonded to the rhodium centers in the supported complex: the Rh–C coordination number ( $N_{\text{Rh–C}}$ ) was found to be 3.9, with a Rh–C distance ( $R_{\text{Rh–C}}$ ) of 2.09 Å. These data indicate two ethylene ligands per Rh atom in the complex, on average. For comparison, the Rh–C distance in the precursor complex  $\text{Rh}(\text{C}_2\text{H}_4)_2(\text{acac})$  in the crystalline state is 2.13 Å.<sup>30–32</sup>

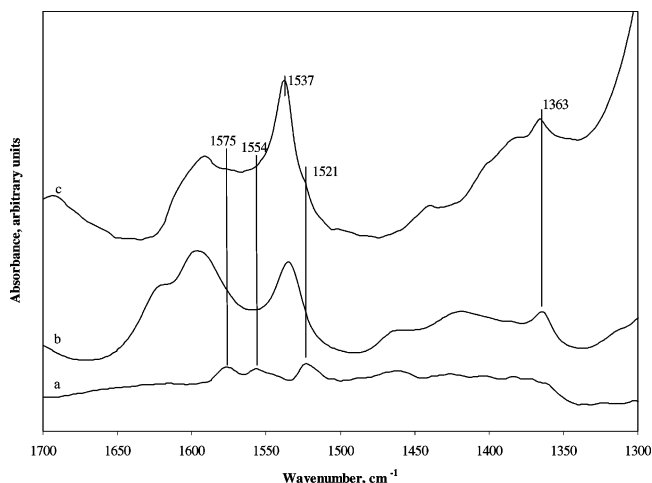


**Figure 5.** IR spectra in the region 1300–1700  $\text{cm}^{-1}$  characterizing the following samples: (a)  $\text{Rh}(\text{C}_2\text{H}_4)_2(\text{acac})$ , (b) sample formed by reaction of DAY zeolite with Hacac, and (c) sample formed by contacting of DAY zeolite with  $\text{Rh}(\text{C}_2\text{H}_4)_2(\text{acac})$ .

**Reaction of acac Ligands during Adsorption of  $\text{Rh}(\text{C}_2\text{H}_4)_2(\text{acac})$ .** Figure 5 provides a comparison of the IR spectra characterizing (1) the 1300–1700  $\text{cm}^{-1}$  region of the precursor  $\text{Rh}(\text{C}_2\text{H}_4)_2(\text{acac})$ , (2) the sample formed by adsorption of this complex on the zeolite, and (3) the surface species formed by adsorption of acetylacetone (Hacac) from *n*-pentane onto the support. The spectrum of crystalline  $\text{Rh}(\text{C}_2\text{H}_4)_2(\text{acac})$  includes strong bands at 1575, 1554, and 1521  $\text{cm}^{-1}$ , which were assigned to  $\nu_s(\text{CO})_{\text{ring}}$ ,  $2[\gamma(\text{C–H})]$ , and  $\nu_{\text{as}}(\text{CCC})_{\text{ring}}$ , respectively.<sup>33</sup> The spectrum of the sample incorporating the supported rhodium complex includes bands at 1591, 1537, and 1363  $\text{cm}^{-1}$ , and this spectrum is similar to that of the sample formed by adsorption of Hacac on the support. Specifically, the bands corresponding to  $\nu_s(\text{CO})_{\text{ring}}$  and  $\nu_{\text{as}}(\text{CCC})_{\text{ring}}$ , which are inferred on the basis of ligand field theory to be more likely than the other bands to be influenced by the metal ion bonded to the acac ligand in the supported complex, match well with the sample formed by Hacac adsorption on the support.<sup>34–36</sup> This comparison indicates dissociation of acac from the rhodium in the supported species.

Moreover, the IR spectrum in the 1300–1700  $\text{cm}^{-1}$  region characterizing the sample formed from  $\text{Rh}(\text{C}_2\text{H}_4)_2(\text{acac})$  and the zeolite nearly matches that of a sample formed from  $\text{Rh}(\text{CO})_2(\text{acac})$  and DAY zeolite, represented as  $\text{Rh}(\text{CO})_2\{\text{OZ}\}_2$  (the results are shown in Supporting Information, Figure 1).<sup>7</sup> The supported sample formed from  $\text{Rh}(\text{CO})_2(\text{acac})$  was characterized by IR and EXAFS spectroscopies and by density functional theory,<sup>7</sup> and the results led to the inferences that the acac ligand was dissociated from the precursor and the resulting complex ( $\text{Rh}(\text{C}_2\text{H}_4)_2$ ) was bonded to the zeolite at T4 sites near aluminum centers.<sup>37</sup>

#### Structure of the Supported Rhodium–Ethylene Complex.

In summary, the data show that the acac ligands of the precursor complex  $\text{Rh}(\text{C}_2\text{H}_4)_2(\text{acac})$  reacted, leaving the ethylene ligands bonded to the rhodium anchored to the support. The supported complex is represented as  $\text{Rh}\{\text{OZ}\}_2(\text{C}_2\text{H}_4)_2$ , where OZ is part of the zeolite framework. This is formally a 16-electron complex, with the OZ group represented as a two-electron donor analogous, for example, to  $\text{Rh}(\text{CO})_2(\text{acac})$ . A schematic representation of the supported rhodium ethylene complex is shown in Figure 6.

**Reactions of Zeolite-Supported Rhodium Complex.** *Reaction with CO.* Figure 7 shows the development of bands in the

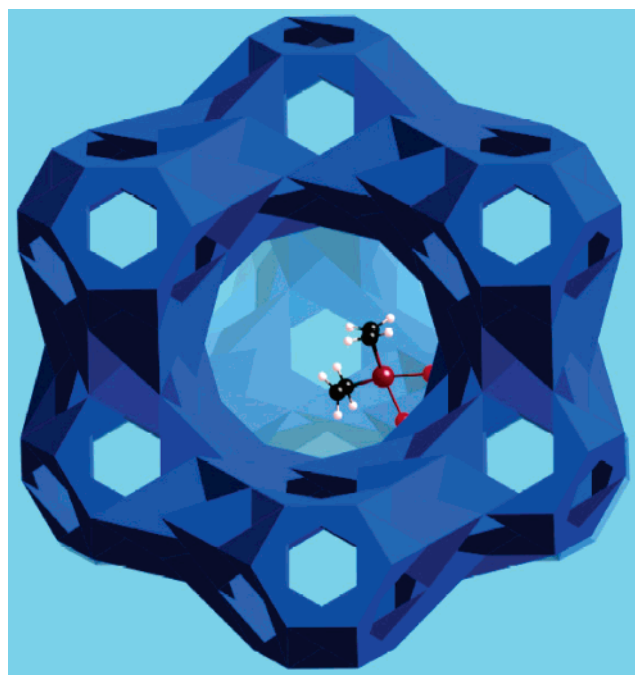


**Figure 6.** Representation of the zeolite-supported rhodium complex formed from  $\text{Rh}(\text{C}_2\text{H}_4)_2(\text{acac})$  and DAY zeolite, in which the Rh atom is bonded to two oxygen atoms from the zeolite framework. The framework of the zeolite is represented only schematically, and the bonding positions of the rhodium complexes in the zeolite are not known.

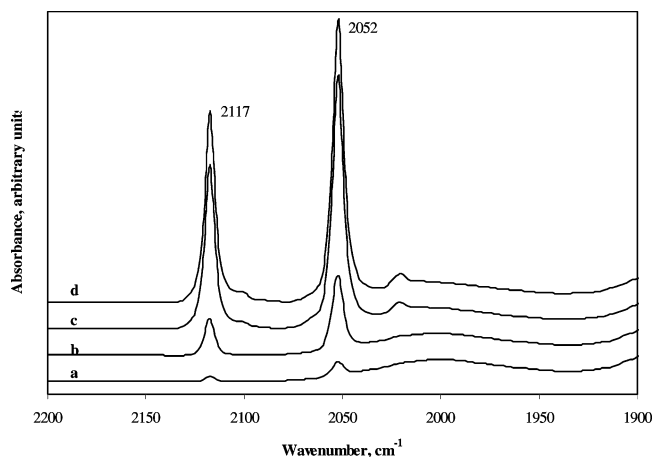


**Figure 7.** IR spectra in the  $\nu_{\text{CO}}$  region of sample formed from DAY zeolite and  $\text{Rh}(\text{C}_2\text{H}_4)_2(\text{acac})$  after interaction with 10 Torr of CO at 298 K for (a) 1.5, (b) 6, (c) 15, and (d) 30 min.

$\nu_{\text{CO}}$  region as the supported rhodium complex was in contact with flowing CO. The formation of narrow IR bands at 2117 and 2052  $\text{cm}^{-1}$  started once the CO flow began at 298 K,<sup>38</sup> indicating the formation of geminal rhodium carbonyl. There was a concomitant decrease in intensities of the bands at 3086, 3015, and 2980  $\text{cm}^{-1}$  accompanied by the disappearance of the  $\nu_{\text{CH}}$  band at 3060  $\text{cm}^{-1}$ , indicating that ethylene ligands were no longer bonded to the rhodium. The fwhm of the carbonyl bands was less than 8  $\text{cm}^{-1}$ , indicating nearly uniform rhodium carbonyl species in the zeolite and suggesting that they may be represented as  $\text{Rh}(\text{CO})_2\{\text{OZ}\}_2$ , although the suggestion that the rhodium is bonded to two oxygen atoms of the zeolite is untested for this sample. This result agrees well with data characterizing a supported rhodium complex formed from  $\text{Rh}(\text{CO})_2(\text{acac})$  and DAY zeolite.<sup>7</sup> The results lead to the inference that the supported

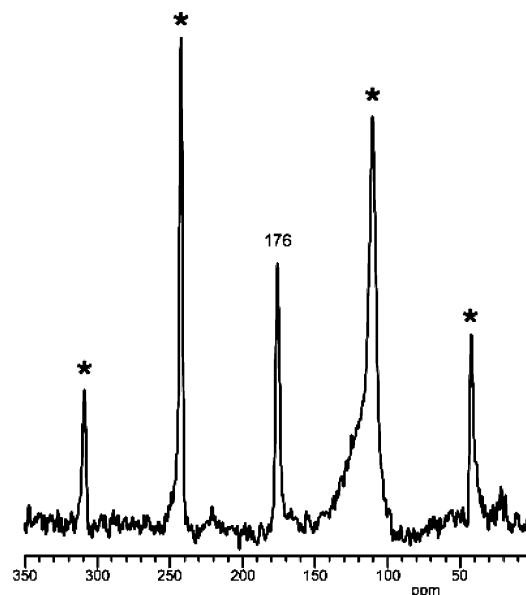


**Figure 8.** 75.4 MHz  $^{13}\text{C}$  Bloch decay MAS NMR spectra of sample formed from  $\text{Rh}(\text{acac})(\text{C}_2\text{H}_4)_2$  with DAY zeolite after treatment with  $^{13}\text{CO}$  (\* denotes spinning sideband).

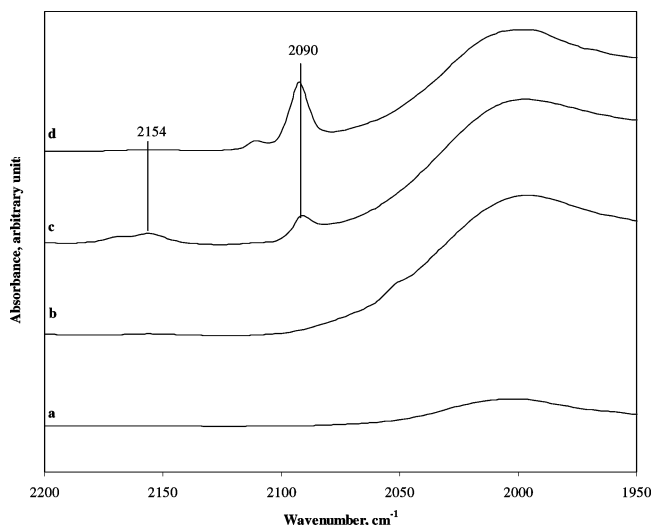


**Figure 9.** IR spectra in the  $\nu_{\text{CO}}$  region characterizing the following samples: (a) DAY zeolite calcined at 773 K, (b) sample formed by reaction of DAY zeolite with  $\text{Rh}(\text{C}_2\text{H}_4)_2(\text{acac})$ , (c) sample b after treatment with  $\text{H}_2$  for 30 min at 298 K, and (d) sample b after treatment with  $\text{D}_2$  at 298 K.

rhodium complexes with ethylene complexes, from which the rhodium carbonyls formed, were also nearly uniform.

The  $^{13}\text{C}$  MAS NMR spectrum (Figure 8) of the  $^{13}\text{C}$ -labeled sample provides further evidence of site-isolated rhodium dicarbonyls bonded to the support. The peak at  $\delta = 176$  ppm along with multiple spinning sidebands is consistent with the formation of isolated  $\text{Rh}(\text{I})(\text{CO})_2$  bonded to the support.<sup>39–42</sup> No other carbon signals are evident in the spectrum.

**Reaction with  $\text{H}_2$ .** Figure 9 shows the development of IR bands when  $\text{H}_2$  was brought in contact with the supported rhodium–ethylene complex at 298 K. The  $\nu_{\text{CH}}$  bands at 3086 and 3015  $\text{cm}^{-1}$  decreased and the band at 3060  $\text{cm}^{-1}$  representing the ethylene ligands bonded to rhodium disappeared during the flow of  $\text{H}_2$  at a partial pressure of 100 Torr in He (Figure 3), with the evolution of ethane in the gas phase, which was identified by gas chromatographic analysis of the effluent stream. Evidently, the ethylene ligands were hydrogenated in

the presence of gas-phase  $\text{H}_2$ . This observation suggests a role of these ligands as intermediates in catalytic hydrogenation of ethylene.

As the ethylene ligands were hydrogenated, a relatively narrow band arose in the IR spectrum at  $2090\text{ cm}^{-1}$ , followed by the appearance of weak broad bands centered at about  $2154$  and  $2168\text{ cm}^{-1}$  (Figure 9). The bands that grew in are different from those that formed when the sample was exposed to 10% CO in He and do not correspond to the formation of geminal carbonyls of rhodium; they remain to be assigned.

To test the hypothesis that the band at  $2090\text{ cm}^{-1}$  was indicative of a rhodium hydride species (expected in the range of  $1800\text{--}2200\text{ cm}^{-1}$ ), we exposed the sample (prior to hydrogenation) to flowing  $\text{D}_2$ . Again, the  $2090\text{ cm}^{-1}$  band formed (Figure 9). Thus, the results rule out the assignment of the  $2090\text{ cm}^{-1}$  band to rhodium hydride.

Instead, the new bands could be indicative of rhodium carbonyls, although it is not evident how they might have formed; CO could have formed from the reactions of the acac ligands on the support.

**Stability in He.** IR spectra characterizing the supported rhodium complex during treatment in He at increasing temperatures up to  $373\text{ K}$  show that the ethylene ligands remained bonded to the rhodium. There was no observable change in intensity of the bands in the  $\nu_{\text{CH}}$  region during this treatment.

**Ethylene Hydrogenation Catalyzed by Supported Rhodium Complex.** The zeolite-supported rhodium complex formed from  $\text{Rh}(\text{C}_2\text{H}_4)_2(\text{acac})$  was found to catalyze ethylene hydrogenation at  $294\text{ K}$  in the presence of 30 Torr of  $\text{H}_2$  and 30 Torr of  $\text{C}_2\text{H}_4$  (in He). The total flow rate was  $100\text{ mL min}^{-1}$ , and the initial reaction rate, measured from a low differential conversion, was found to be  $0.022\text{ (mmol C}_2\text{H}_4) \times \text{s}^{-1} \times (\text{mmol of Rh})^{-1}$ .<sup>43</sup>

The catalyst lost activity during operation in the flow reactor, with the reaction rate declining to a steady-state value of  $2.1 \times 10^{-3}\text{ (mmol of C}_2\text{H}_4) \times \text{s}^{-1} \times (\text{mmol of Rh})^{-1}$  after 18 h on stream (Supporting Information, Figure 2). Subsequently, when the  $\text{H}_2$  partial pressure was increased from 30 to 300 Torr with the total flow rate held constant at  $100\text{ mL min}^{-1}$  (by lowering the partial pressure of He), the catalytic activity increased 4-fold within an hour and was stable for 2 h before catalyst deactivation was apparent.

## Discussion

**Synthesis of Supported Metal Complexes with Ethylene Ligands.** The goal of preparing supported metal complexes with only ethylene ligands (in addition to the support ligands) is appealing because of the opportunities that such complexes offer for fundamental investigations of the reactivities of site-isolated metal–ethylene complexes and their role as possible catalytic intermediates. The reactivity of the precursor with the support is influenced both by the groups present on the support and the nature of the metal atom in the precursor.<sup>34,36,44</sup>

Earlier reports of attempts to synthesize supported rhodium complexes with alkene ligands have led to less than well-defined structures. For example, Schneider et al.<sup>45</sup> preceded us in using  $\text{Rh}(\text{C}_2\text{H}_4)_2(\text{acac})$  as a precursor of supported rhodium complexes. As supports, they used  $\text{SiO}_2$  and  $\text{MgO}$  that had high surface concentrations of OH groups. They suggested that the precursor–support reactions occurred analogously to the reaction between  $\text{Rh}(\eta^3\text{-C}_3\text{H}_5)_3$  and OH groups of  $\text{SiO}_2$ , which forms a supported bis(allyl)rhodium complex and a molecule of propene,<sup>46–48</sup> but data characterizing the reaction and the resultant surface species are lacking. In contrast, Gbureck et

al.<sup>49</sup> found that the precursor  $\text{Rh}(\text{C}_2\text{H}_4)_2(\text{acac})$  remained intact on their  $\text{SiO}_2$  support, being only weakly bonded to the oxygen atoms of the support OH groups, as evidenced by  $\nu_{\text{CH}}$  bands in the Raman spectrum. Such weak surface–metal complex interactions may be attributed to van der Waals forces. In contrast, stronger interactions are needed for reactions such as those observed in our experiments.

Thus, the work of Schneider et al.<sup>45</sup> and of Gbureck et al.<sup>49</sup> is contrasted to our preparation of a structurally almost uniform rhodium complex on the zeolite resulting from selective reaction of the acac ligands without breaking of the rhodium–ethylene bonds. One reason for the success of our preparation is inferred to be the relatively low concentration of OH groups on the surface of our support (consistent with the results of Bhirud et al. for a  $\text{MgO}$ -supported rhodium complex<sup>10</sup>).

Other attempts to prepare supported rhodium complexes with alkene ligands have led to surface species with ligands other than alkene on the rhodium, including chloride and phosphine,<sup>50,51</sup> which complicate the structural characterization.

Our results are comparable to those of Van Der Voort,<sup>44</sup> who showed that in the reaction of  $\text{VO}(\text{acac})_2$  with pure-silica MCM-48 some of the acac ligands undergo ligand exchange, becoming bonded to oxygen atoms of the support, and some become bonded to the support by hydrogen-bond interactions. Another example involving comparable surface chemistry is the reaction between  $\text{Au}(\text{CH}_3)_2(\text{acac})$  and partially dehydroxylated  $\gamma\text{-Al}_2\text{O}_3$ , which led to the formation of dimethyl–gold complexes bonded to the support and to surface  $\text{Al}(\text{acac})_3$  groups, formed from the dissociated acac ligands, as shown by IR spectroscopy.<sup>52</sup>

The important result for the synthesis of the supported rhodium–ethylene complex is that the acac ligands react more readily with the support surface than the ethylene ligands. The literature of molecular complexes of rhodium is not sufficient to have predicted this result, although it gives some hints. For example, ethylene in  $(\pi\text{-C}_5\text{H}_5)\text{Rh}(\text{C}_2\text{H}_4)_2$  is displaced in a bimolecular reaction by weak Lewis acids (e.g.,  $\text{SO}_2$ ),<sup>53</sup> but the reaction occurs at substantial rates only at temperatures above  $388\text{ K}$ , well in excess of that used in our preparation and in others<sup>34,36,52</sup> in which acac ligands in metal complexes react with oxide and zeolite surfaces.

**Reactivity and Uniformity of Supported Rhodium Complexes.** The observed reactivities of the supported rhodium–ethylene complex are broadly consistent with the chemistry of rhodium–ethylene complexes in solution. For example, formation of the rhodium carbonyl upon exposure of the surface rhodium–ethylene complex to CO leads to the well-known rhodium gem-dicarbonyl species bonded to the support;<sup>7</sup> such species are quite stable and formed from numerous precursors.<sup>7,22,54</sup> The sharpness of the carbonyl bands (with fwhm of less than  $8\text{ cm}^{-1}$ ) compares well with the sharpness of the bands (fwhm of less than  $5\text{ cm}^{-1}$ ) observed by Miessner et al.<sup>22</sup> and is evidence of the near uniformity of the rhodium species on the support. The reaction of the supported rhodium–ethylene complex with  $\text{H}_2$  to form ethane is similar to chemistry occurring in the Wilkinson catalytic hydrogenation of alkenes<sup>55</sup> and suggests the likelihood that the surface complex is an intermediate in the catalytic cycle for ethylene hydrogenation.

**Catalytic Performance.** The supported rhodium–ethylene complex is one of a number of such complexes that are precursors of catalysts for hydrogenation. Examples include silica- and ultrastable Y zeolite-supported complexes formed from  $\text{Rh}[\text{Cl}(\text{COD})\text{L}]$ , where COD is cyclooctadienyl and L is 2(3-triethoxysilylpropyl)aminocarbonylpyrrolidine; these preparations give surface species that are less than fully character-



ized.<sup>56</sup> Furthermore,  $\gamma$ -Al<sub>2</sub>O<sub>3</sub>-supported catalysts were prepared from physisorbed Rh( $\pi$ -C<sub>3</sub>H<sub>5</sub>)CO(PPh<sub>3</sub>)<sub>2</sub>,<sup>57</sup> and polymer-supported complexes were formed from the reaction of Wilkinson's catalyst RhCl(PPh<sub>3</sub>)<sub>3</sub> (Ph = phenyl) with amide groups of the polymer.<sup>58,59</sup> The rate of ethylene hydrogenation catalyzed by polymer-supported rhodium complex (found by extrapolation of the published data<sup>58</sup>) was  $8 \times 10^{-4}$  (mmol of C<sub>2</sub>H<sub>4</sub>)  $\times$  s<sup>-1</sup>  $\times$  (mmol of Rh)<sup>-1</sup> at 294 K when the partial pressures of ethylene and H<sub>2</sub> were each 209 Torr. Thus, this polymer-supported rhodium complex is 2 orders of magnitude less active than our zeolite-supported rhodium complex at the same temperature and in the presence of lower reactant partial pressures (30 Torr of H<sub>2</sub> and 30 Torr of C<sub>2</sub>H<sub>4</sub>).

Our supported rhodium–ethylene complex is the first that appears to be a good candidate to be an intermediate in a catalytic cycle, but more work is needed to determine whether it is. If it is such an intermediate, the sample provides an opportunity to determine details of the cycle, such as the intermediate hydrocarbons that may be formed from the ethylene ligands and H<sub>2</sub>.

## Conclusions

IR, EXAFS, and <sup>13</sup>C NMR spectroscopies were used to characterize the structure of a sample formed from the reaction of Rh(C<sub>2</sub>H<sub>4</sub>)<sub>2</sub>(acac) with DAY zeolite. EXAFS data demonstrate that the supported rhodium complex is mononuclear with each Rh center bonded on average to two oxygen atoms of the support with a Rh–O distance of 2.19 Å. IR, <sup>13</sup>C NMR, and EXAFS spectra indicate that the ethylene ligands remained bonded to the Rh centers. The supported rhodium complex was found to catalyze ethylene hydrogenation at 294 K.

**Acknowledgment.** This research was supported by the U.S. Department of Energy (DOE), Grants DE-FG02-04ER15598 and DE-FG02-04ER15600. We acknowledge beam time and the support of the DOE Division of Materials Sciences for its role in the operation and development of beamline X-18B at the National Synchrotron Light Source. We also acknowledge the Stanford Synchrotron Radiation Laboratory, which is operated by Stanford University for the U.S. Department of Energy, Office of Basic Energy Science, for access to beam time on beamline 2-3. We are grateful to the beamline staff at both facilities for their assistance.

**Supporting Information Available:** IR spectra comparing supported rhodium–ethylene and rhodium–carbonyl complexes; plot showing break-in of catalyst in a flow reactor; and plot of EXAFS data and fits illustrating the goodness of fit and the residuals remaining after the fit. The material is available free of charge via the Internet at <http://pubs.acs.org>.

## References and Notes

- (1) Cop  ret, C.; Chabanas, M.; Saint-Arroman, R. P.; Basset, J.-M. *Angew. Chem., Int. Ed.* **2003**, *42*, 156.
- (2) Guzman, J.; Gates, B. C. *Dalton Trans.* **2003**, 3303.
- (3) Hlatky, G. G. *Chem. Rev.* **2000**, *100*, 1347.
- (4) Yoneda, N.; Shiroto, Y.; Hamoto, K.; Asaoka, S.; Maejima, T. U.S. Patent 5334755.
- (5) Yoneda, N.; Kusane, S.; Yasui, M.; Pujado, P.; Wilcher, S. *Appl. Catal., A* **2001**, *221*, 253.
- (6) Cop  ret, C.; Maury, O.; Thivolle-Cazat, J.; Basset, J.-M. *Angew. Chem., Int. Ed.* **2001**, *40*, 2331.
- (7) Goellner, J. F.; Gates, B. C.; Vayssilov, G. N.; R  sch, N. *J. Am. Chem. Soc.* **2000**, *122*, 8056.
- (8) Van Der Voort, P.; White, M. G.; Vansant, E. F. *Langmuir* **1998**, *14*, 106.
- (9) Guzman, J.; Gates, B. C. *J. Phys. Chem. B* **2002**, *106*, 7659.
- (10) Bhirud, V. A.; Ehresmann, J. O.; Kletnieks, P. W.; Haw, J. F.; Gates, B. C. *Langmuir*, in press.
- (11) Xu, T.; Haw, J. F. *Top. Catal.* **1997**, *4*, 109.
- (12) Jentoft, R. E.; Deutsch, S. E.; Gates, B. C. *Rev. Sci. Instrum.* **1996**, *67*, 2111.
- (13) Odzak, J. F.; Argo, A. M.; Lai, F. S.; Gates, B. C.; Pandya, K.; Feraria, L. *Rev. Sci. Instrum.* **2001**, *72*, 3943.
- (14) Newville, M. *J. Synchrotron Rad.* **2001**, *8*, 322.
- (15) Vaarkamp, M.; Linders, J. C.; Koningsberger, D. C. *Physica B* **1995**, *209*, 159.
- (16) Zabinsky, S. I.; Rehr, J. J.; Ankudinov, A.; Albers, R. C.; Eller, M. J. *Phys. Rev. B* **1995**, *52*, 2995.
- (17) Duivenvoorden, F. B. M.; Koningsberger, D. C.; Uh, Y. S.; Gates, B. C. *J. Am. Chem. Soc.* **1986**, *108*, 6254.
- (18) Kirlin, P. S.; van Zon, F. B. M.; Koningsberger, D. C.; Gates, B. C. *J. Phys. Chem. B* **1990**, *94*, 8439.
- (19) van Zon, J. B. A. D.; Koningsberger, D. C.; van't Blik, H. F. J.; Sayers, D. E. *J. Chem. Phys.* **1985**, *82*, 5742.
- (20) Guzman, J.; Gates, B. C. *J. Catal.* **2004**, *226*, 111.
- (21) Lytle, F. W.; Sayers, D. E.; Stern, E. A. *Physica B* **1989**, *158*, 701.
- (22) Miessner, H.; Burkhardt, I.; Gutschick, D.; Zecchina, A.; Morterra, C.; Spoto, G. *J. Chem. Soc., Faraday Trans.* **1989**, *85*, 2113.
- (23) Koningsberger, D. C.; Gates, B. C. *Catal. Lett.* **1992**, *14*, 271.
- (24) Cramer, R. J. *Am. Chem. Soc.* **1964**, *86*, 217.
- (25) The weak band with a negative intensity at about 3000 cm<sup>-1</sup> is the result of subtraction of the background spectrum collected with the evacuated cell from the spectrum of the sample formed by adsorption of the rhodium ethylene complex on the zeolite.
- (26) Vierk  tter, S. A.; Barnes, C. E. *J. Am. Chem. Soc.* **1994**, *116*, 7445.
- (27) Detailed NMR investigations of ethylene adsorbed on acidic sites in zeolites<sup>28,29</sup> indicate that the <sup>13</sup>C resonance in such complexes is close to its gas-phase value of >120 ppm, and therefore such an assignment does not explain the 60 ppm resonance.
- (28) White, J. L.; Beck, L. W.; Haw, J. F. *J. Am. Chem. Soc.* **1992**, *114*, 6182.
- (29) Munson, E. J.; Kheir, A. A.; Lazo, N. D.; Haw, J. F. *J. Phys. Chem. B* **1992**, *96*, 7740.
- (30) Evans, J. A.; Russell, D. R. *J. Chem. Soc., Chem. Commun.* **1971**, 197.
- (31) B  hl, M.; H  kansson, M.; Mahmoudkhani, A. H.;   hrstr  m, L. *Organometallics* **2000**, *19*, 5589.
- (32) Cramer, R. *Inorg. Synth.* **1974**, *15*, 14.
- (33) Because of the spectral quality, we were unable to observe the weaker bands present for the crystalline complex. The better-quality spectrum reported by Cramer<sup>32</sup> shows bands for this complex at 3060 (w), 2985 (w), 1575 (s), 1558 (s), 1524 (s), 1425 (m), 1372 (m), 1361 (m), 1267 (m), 1233 (m), 1221 (w), 1199 (w), and 1015 cm<sup>-1</sup> (w).
- (34) Van Der Voort, P.; Mathieu, M.; Vansant, E. F.; Rao, S. N. R.; White, M. G. *J. Porous Mater.* **1998**, *5*, 305.
- (35) Van Der Voort, P.; Babitch, I. V.; Grobet, P. J.; Verberckmoes, A. A.; Vansant, E. F. *J. Chem. Soc., Faraday Trans.* **1996**, *92*, 3635.
- (36) Van Der Voort, P.; van Welzenis, R.; de Ridder, M.; Brongersma, H. H.; Baltes, M.; Mathieu, M.; van de Ven, P. C.; Vansant, E. F. *Langmuir* **2002**, *18*, 4420.
- (37) Because of the width of peaks corresponding to acac, the IR spectra do not determine whether all the precursor acac groups reacted.
- (38) The minor bands at 2100 and 2021 cm<sup>-1</sup> correspond to the <sup>13</sup>CO in natural abundance and are visible because of the sharpness of the main peaks.<sup>22</sup>
- (39) Brown, C.; Heaton, B. T.; Longhetti, L.; Poley, W. T.; Smith, D. O. *J. Organomet. Chem.* **1986**, *192*, 93.
- (40) Takahashi, N.; Miura, K.; Fukui, H. *J. Phys. Chem.* **1986**, *90*, 2797.
- (41) Weber, W. A.; Phillips, B. L.; Gates, B. C. *Chem.—Eur. J.* **1999**, *5*, 2899.
- (42) Molitor, P. F.; Shoemaker, R. K.; Apple, T. M. *J. Phys. Chem. B* **1989**, *93*, 2891.
- (43) The only product observed was ethane, and there was no measurable conversion of ethylene and hydrogen in the absence of catalyst or in the presence of the support alone under the conditions of the experiments.
- (44) Van Der Voort, P.; Morey, M.; Stucky, G. D.; Mathieu, M.; Vansant, E. F. *J. Phys. Chem. B* **1998**, *102*, 585.
- (45) Schneider, M. E.; Mohring, U.; Werner, H. *J. Organomet. Chem.* **1996**, *520*, 181.
- (46) Basset, J.-M.; Dufour, P.; Houtman, C.; Santini, C. C.; Hsu, L.; Shore, S. *J. Am. Chem. Soc.* **1992**, *114*, 4248.
- (47) Dufour, P.; Scott, S. L.; Santini, C. C.; Lefebvre, F.; Basset, J.-M. *Inorg. Chem.* **1994**, *33*, 2509.
- (48) Scott, S. L.; Basset, J.-M.; Niccolai, G. P.; Santini, C. C.; Candy, J.-P.; Lecuyer, C.; Quignard, F.; Choplin, A. *New J. Chem.* **1994**, *18*, 115.
- (49) Gbureck, A.; Kiefer, W.; Schneider, M. E.; Werner, H. *Vib. Spectrosc.* **1998**, *17*, 105.
- (50) Kinting, A.; Krause, H.; Capka, M. *J. Mol. Catal.* **1985**, *33*, 215.

- (51) Michalska, Z. M.; Capka, M.; Stoch, J. *J. Mol. Catal.* **1981**, *11*, 323.
- (52) Guzman, J.; Gates, B. C. *Langmuir* **2003**, *19*, 3897.
- (53) Cramer, R. *J. Am. Chem. Soc.* **1972**, *94*, 5681.
- (54) Miessner, H.; Gutschick, D.; Ewald, H.; Müller, H. *J. Mol. Catal.* **1986**, *36*, 359.
- (55) Young, J. F.; Osborn, J. A.; Jardine, F. H.; Wilkinson, G. *J. Chem. Soc., Chem. Commun.* **1965**, 131.
- (56) Sanchez, F.; Iglesias, M.; Corma, A.; Del Pino, C. *J. Mol. Catal.* **1991**, *70*, 369.
- (57) Spek, T. G.; Scholten, J. J. F. *J. Mol. Catal.* **1977**, *3*, 81.
- (58) Uematsu, T.; Nakazawa, Y.; Akutsu, F.; Shimazu, S.; Miura, M. *Makromol. Chem. Commun.* **1987**, *188*, 1085.
- (59) Kim, T. H.; Rase, H. F. *Ind. Eng. Chem. Prod. Res. Dev.* **1976**, *15*, 249.